revista mexicana de física 26 no. 2 (1979) 155-188

SUBBAND STRUCTURE OF SEMICONDUCTING SURFACE SPACE CHARGE LAYERS *

John J. Quinn

Brown University,

Providence, Rhode Island 02912, USA

ABSTRACT

The electric subband structure of semiconducting surface accumulation or inversion layers is studied. Hartree variational functions are used as basis states for a many-body perturbation theory. The exchange and correlation contributions to the quasi-particle energies are evaluated as a function of electron concentration and temperature. The effects of resonant screening and final state interactions on the intersubband optical absorption are investigated for the case of zero temperature. - Surface channel tunneling experiments which should give direct information on quasi-particle separations are described.

RESUMEN

Se estudia la estructura de sub-banda de capas de acumulación e inversión en superficies de semiconductores. Se usan funciones variacionales de Hartree como estados de base para una teoría de perturbaciones de muchos cuerpos. Las contribuciones de intercambio (exchange) y correlación a las energías de las cuasi-partículas son evaluadas como función de la concentración electrónica y de la temperatura. Los efectos de apantallamiento resonante y de interacciones de estado final sobre la absorción óptica en la sub-banda son investigadas para el caso de temperatura cero. Se describen experimentos de tunelamiento a través de "canales de superficie".

INTRODUCTION

The surface potential well formed when an attractive electric field is applied normal to the surface of a semiconductor can give rise to quantization of the motion of electrons normal to the surface. Because the electrons are free to move parallel to the surface, each quantized

---

* Supported in part by the National Science Foundation and by the Office of Naval Research.

level of the surface potential well forms a two-dimensional energy band referred to as an electric subband. The study of the subband structure of surface accumulation and inversion layers has proved to be an interesting problem. The first calculations[1,2] of the subband structure were made using the Hartree approximation. Comparison of these calculations with the early observations of intersubband optical absorption[3,4] made it quite clear that the effects of exchange and correlation were very important. Stern[5] evaluated the exchange energy and showed that it lowered the energy of the ground subband by a substantial amount. Vinter[6] calculated the self-energies of electrons in different subbands by starting with the self-consistent Hartree solution and using many-body perturbation theory. Ando[7] has evaluated the subband structure using a density functional formulation based on the Hohenberg, Kohn and Sham[8,9] theory of an inhomogeneous electron gas. Both Vinter and Ando restrict their consideration to the case of zero temperature when only the ground subband is occupied. Recently Kalia *et al*[10] have extended the many-body perturbation theory to the case of finite temperatures. Kneschaurek and Koch[11] have performed the first studies of the temperature dependence of the intersubband absorption.

One might ask why there has been so much effort devoted to the subband structure of surface space charge layers. The reason is that such systems are extremely interesting many-body systems. The electron concentration in a surface inversion layer can be varied over a wide range of values simply by changing the surface electric field. Because exchange and correlation effects depend very strongly on the electron concentration, one can pass from a very weakly interacting many-body system (at a very high electron density) to a strongly interacting one. In addition, the Fermi temperature of the quasi-two-dimensional electron gas of a surface inversion layer is of the order of 10^1 to 10^2°K. Thus, one can pass from a highly degenerate electron gas at very low temperature to a nondegenerate gas at room temperature and study how correlation effects depend on temperature. Finally, many-body effects are relatively more important in these quasi-two-dimensional systems than in bulk solids. The Hartree energy separations are of the order of 10 meV, and it turns out that correlation effects can be as large or larger.

It is well-known that the quasi-two-dimensional layer compounds ex-

hibit charge and spin density wave instabilities[12]. It appears to be likely that some unusual properties of inversion layers are associated with charge density wave type instabilities[13].

In this paper we review the Hartree approximation for the subband structure, making use of approximate variational wave functions to avoid excessive numerical calculation. The finite temperature many-body perturbation theory is discussed in some detail, and results for quasi-particle energies as a function of temperature and inversion layer concentration are presented[10]. In order to compare the optical absorption experiments with the calculated quasi-particle separations, two additional effects must be included: the depolarization effect or resonant screening and the final state interaction or vertex correction. Both of these effects are studied by many-body perturbation theory for the case of zero temperature[14], and a large cancellation is found. This agrees qualitatively with the result of Ando[15] who used a very different method of calculation and different approximations. Finally, a new experimental technique for directly observing the quasi-particle separations is discussed, the technique of surface channel tunneling[16]. -- This technique should make it possible to compare directly the experimental data and the calculated quasi-particle energies.

I. THE METAL-INSULATOR-SEMICONDUCTOR STRUCTURE

In actual metal-insulator-semiconductor (MIS) structures a number of subtle but important effects are caused by complicated details of the semiconductor band structure like valley degeneracy, nonparabolicity and anisotropy. Since the basic physics of the MIS structure can be understood without these complications, we consider first a simple model semiconductor whose valence and conduction band energies are given by

$$E_V = -E_G - \hbar^2 k^2/2m_V \quad (1)$$

$$E_C = \hbar^2 k^2/2m_C \quad (2)$$

Here $\vec{k}$ is the wavevector measured from the Γ-point, the center of the Brillouin zone.

In an n-type semiconductor there are a number of donor states whose energy is in the band gap just slightly below the conduction band edge. At zero temperature the donors will be neutral, i.e., the extra electron of the donor atom will be bound in a hydrogen like orbit to the donor ion. The binding energy is given roughly by

$$E_D \simeq - e^4 m_c / 2\hbar^2 \varepsilon_s^2 , \tag{3}$$

where ε_s is the dielectric constant of the semiconductor. This is smaller by a factor of $m_c/m_o\varepsilon_s^2$ than the Rydberg, where m_o is the mass of a free electron. Typical values of this factor are of the order of 10^{-3}, so that donor binding energies are of the order of 10meV. Because this binding energy is small, many donors can be ionized at finite temperatures,donating their extra electron to the conduction band. A similar picture holds for acceptor states if holes replace electrons and valence band replaces conduction band.

To be explicit we shall consider an ideal semiconductor with N_A acceptors and N_D donors per unit volume with $N_A > N_D$ so that the material is p-type. At zero temperature all of the donor states will be ionized. The extra electron from each donor state will be captured by an acceptor, so that N_D of the acceptors will be ionized and $N_A - N_D$ will be neutral. The valence band is completely filled and the conduction band completely empty. Clearly the Fermi energy must be at the acceptor levels since these are partially occupied at zero temperature.

We now consider the MIS structure shown in Fig. 1. An insulating layer of thickness δ and dielectric constant ε_0 separates our ideal semiconductor from a metallic gate electrode. For the moment we can disregard the degenerate n-type source and drain contacts shown in the figure. If electrical contact is established between the metal and the semiconductor, their Fermi levels will attain the same value as shown in Fig. 2. When a voltage is applied between the metal and the semiconductor, there will be an electric field in the insulating layer. Because the normal component of $\vec{D} = \varepsilon\vec{E}$ must be continuous at the semiconductor-insulator interface, the electric field will not be confined to the insulator, but will penetrate into the semiconductor. In the presence of an electric

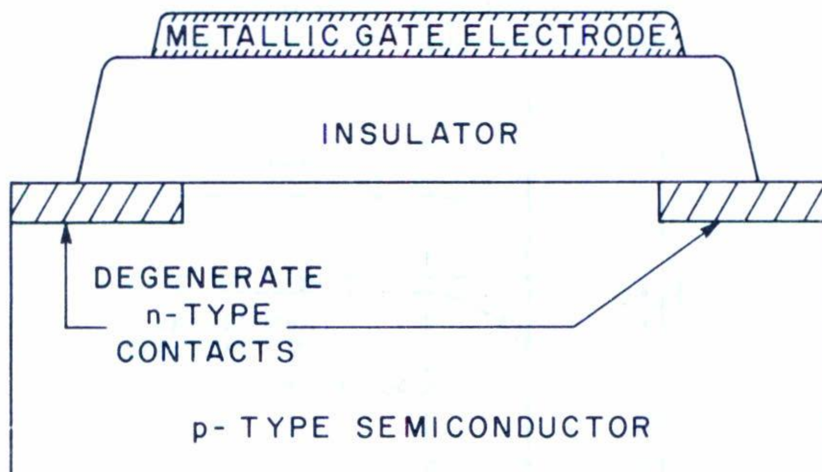

Fig. 1. Schematic MIS structure used for inversion layer experiments. The number of inversion layer electrons per cm^2 of surface is changed by varying the voltage between the metallic gate and the semiconductor. The degenerate n-type source and drain contacts are connected by the surface inversion layer. A small potential difference between source and drain contact leads to a surface current which depends upon the conductance of the inversion layer.

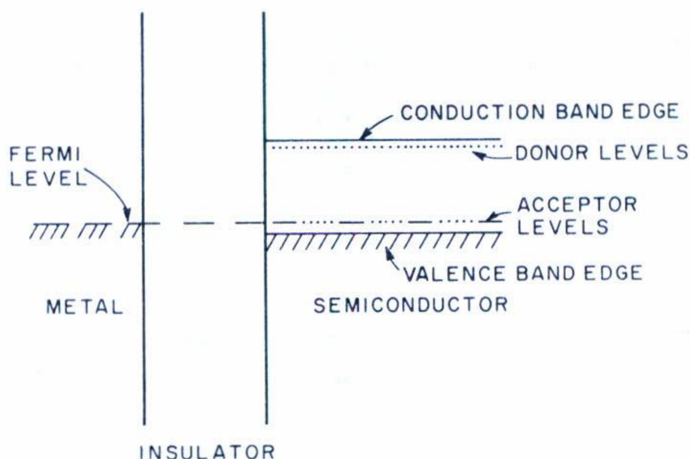

Fig. 2. Schematic of the energy bands along a line normal to the MIS surfaces. The Fermi level is shown as a dashed line. In the semiconductor, which is weakly p-type, the Fermi level lies in the band gap just above the valence band edge at the position of the partially occupied acceptor levels. The insulator has a large band gap, and it has no conducting states in the vicinity of the Fermi level.

field the energy bands of the semiconductor (and the donor and acceptor levels associated with the band edges) will bend as shown in Fig. 3. The electric field in the semiconductor drops from its value at the interface to zero over a distance d; this region is known as the depletion layer.

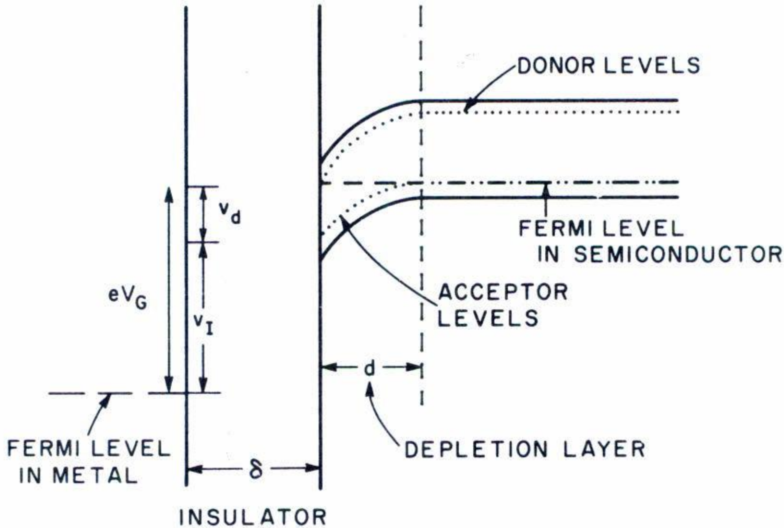

Fig. 3. Schematic of the band structure when a gate voltage is applied. The positive charge density on the surface of the metallic gate electrode leads to a uniform electric field in the insulator (linear potential). The lines of force originating on the surface charges of the gate electrode terminate on negatively charged acceptors in the region of the semiconductor where the bands are bent by the electric field (the depletion layer). For a sufficiently large electric field the conduction band edge at the interface is pulled below the Fermi level of the bulk semiconductor and electrons can be trapped in the surface potential well. In this case the conducting surface channel is called an inversion layer.

In the depletion layer all of the acceptors are ionized since they lie below the Fermi level of the semiconductor. The charge density per unit volume in the depletion layer is simply $- e\ (N_A - N_D)$, since all the acceptors are negatively charged and all the donors positively charged. Beyond the depletion layer charge neutrality prevails. It is convenient

to introduce the potential energy $v_d(z)$ of an electron in the electric field of the depletion layer. The subscript d denotes the association of this potential with the depletion layer charge. The gradient of $v_d(z)$ must be equal to $eE(z)$, where $E(z)$ is the electric field and $-e$ is the charge on an electron. If we take the semiconductor-insulator interface to be the plane $z = 0$, then Poisson's equation in the semiconductor becomes

$$\frac{\partial^2 v_d}{\partial z^2} = -\frac{4\pi e^2}{\varepsilon_s} (N_A - N_D) [1 - \theta(z - d)] \quad (4)$$

Here $\theta(z)$ is a unit step function. Integrating this equation twice with respect to z gives

$$v_d(z) = -\frac{4\pi e^2}{\varepsilon_s} (N_A - N_D)^{1/2} [z^2 - \theta(z - d)(z - d)^2]$$

$$+ v_d' (0) z + v_d(0), \quad (5)$$

where $v_d(0)$ and $v_d'(0)$ are the values of $v_d(z)$ and its first derivative at $z = 0$. We choose the zero of potential to be the value of $v_d(z)$ at $z = \infty$. This fixes the values of $v_d(0)$ and $v_d'(0)$

$$v_d(0) = \frac{-2\pi e^2}{\varepsilon_s} (N_A - N_D) d^2 , \quad (6)$$

$$v_d'(0) = \frac{4\pi e^2}{\varepsilon_s} (N_A - N_D) d \quad . \quad (7)$$

Thus we find

$$v_d(z) = \frac{-2\pi e^2}{\varepsilon_s} (N_A - N_D) (d - z)^2 [1 - \theta(z - d)] \quad (8)$$

Eq. (8) describes the potential energy of an electron in the depletion layer. The charge density in the depletion layer is uniform and equal to $-e(N_A - N_D)$. The width d of the depletion layer increases with increasing voltage so that the charge per unit area of the interface contained in the depletion layer,

$$-eN_d = -e(N_A - N_D)d \ , \tag{9}$$

increases with increasing gate voltage. The electric field in the insulator is constant and given by

$$eE_I = \frac{\varepsilon_s}{\varepsilon_0} v_d'(0) \ , \tag{10}$$

the requirement that the normal component of the displacement field be continuous. The gate voltage (voltage applied between the metallic gate electrode and the semiconductor) is given by

$$eV_G = \frac{4\pi e^2}{\varepsilon_s} N_d \left(\frac{d}{2} + \frac{\varepsilon_s}{\varepsilon_0}\delta \right) \ . \tag{11}$$

As V_G is increased the width of the depletion layer continues to increase until $v_d(0) = -(E_G - E_A)$, where E_A is the binding energy of the acceptors. Since $E_A \ll E_G$, it is often neglected in this expression. For values of V_G larger than this critical value, the conduction band edge at the surface is pulled down below the bulk Fermi level of the semiconductor. In this situation it is possible for electrons to be trapped in the conduction band at the semiconductor-insulator interface. Continuing to increase V_G simply pulls the conduction band edge further and further below the Fermi level in the semiconductor and increases the number of electrons trapped in the conduction band at the surface. The electrons trapped in the conduction band form a conducting n-type surface channel. Since the

bulk semiconductor is p-type, this conducting surface channel is called a surface inversion layer.

The inversion layer electrons contribute to the potential in the semiconductor just as the depletion layer charges do. In fact, we can write down the potential experienced by an electron in the inversion layer as

$$v(z) = v_d(z) + v_s(z) + v_i \quad . \tag{12}$$

Here $v_d(z)$ is the potential due to the depletion charge and is given by Eq. (8) with d approximately equal to $\varepsilon_s E_G / 2\pi e^2 d N_d$. The self-consistent potential of the inversion layer electrons must satisfy the Poisson equation

$$\frac{\partial^2 v_s(z)}{\partial z^2} = \frac{-4\pi e^2}{\varepsilon_s} N_s(z) \quad , \tag{13}$$

where $N_s(z)$ is the electron density in the inversion layer. Finally v_i is the image potential resulting from the difference in dielectric constant between the semiconductor and the insulator. Elementary electrostatics gives

$$v_i(z) \simeq \frac{\varepsilon_s - \varepsilon_o}{4\varepsilon_s(\varepsilon_s + \varepsilon_o)} \frac{e^2}{z} \tag{14}$$

Since ε_s is usually larger than ε_o, the image force is repulsive.

The inversion layer electron density $N_s(z)$ can be written as

$$N_s(z) = N_{inv} \sum_n f(E_n) |\psi_n(z)|^2 \quad , \tag{15}$$

where $\psi_n(z)$ and E_n are the nth eigenfunction and corresponding eigenvalue of the surface potential well. f(E) is the Fermi distribution function and N_{inv} is the number of inversion layer electrons per unit area of the surface.

II. HARTREE APPROXIMATION

The eigenvalues E_n and eigenfunctions $\psi_n(z)$ appearing in Eq. (15) are solutions of the Schrödinger equation

$$[H_o + v(z)]\,\Psi = E\Psi \quad . \tag{16}$$

The potential v(z) is given by Eq. (12), and because it contains the term $v_s(z)$ which depends upon the solutions $\psi_n(z)$ of Eq. (16), the problem must be solved self-consistently. The Hamiltonian H_o appearing in Eq. (16) is actually that for an electron in a perfect crystal. The Bloch functions $\psi_{nk}(r)$ satisfy the equation

$$H_o\psi_{nk}(r) = \varepsilon_n(k)\psi_{nk}(r) \quad . \tag{17}$$

The Bloch functions form a complete orthonormal set

$$\int \psi_{nk}{}^{*}\,\psi_{n'k}\,d\vec{r} = \delta_{nn'}\,\delta_{kk'} \quad , \tag{18}$$

and can be written

$$\psi_{nk}(r) = e^{i\vec{k}\cdot\vec{r}}\,u_{nk}(r) \quad , \tag{19}$$

where $u_{nk}(r)$ has the periodicity of the lattice. Clearly we can expand the wavefunction ψ of Eq. (16) in a series involving Bloch functions

$$\psi(r) = \sum_{nk} A_n(k)\,\psi_{nk}(r) \quad . \tag{20}$$

Because v(z) depends only on z, the motion in the x-y plane is unaffected by the potential v(z) and the problem can be treated as a one-dimensional one.

Single Band Effective Mass Approximation

Substituting Eq. (2) into the Schrödinger Eq. (16), gives a rather complicated problem in the general case. A considerable simplification can be obtained by making the following assumptions:

i) a single band, the conduction band makes the dominant contribution to the wave function $\psi(r)$ given by Eq. (20).

ii) the only important values of $\vec{k}$ in the sum appearing in Eq. (20) come from very close to the single conduction band minimum, which for our simple model is at $k = 0$.

With these assumptions we can write

$$\psi(r) \simeq \sum_{\vec{k}} (k)\, e^{i\vec{k}\cdot\vec{r}}\, u_k(r) \quad , \tag{21}$$

where $u_k(r)$ is the periodic part of the Bloch function for a conduction band state. The Schrödinger equation can be rewritten

$$[\varepsilon(k) - E]\; A(k) + \sum_{k'} < k|v(z)|k' > A(k') = 0 \tag{22}$$

Here $\varepsilon(k)$ is the conduction band energy and

$$<k|v(z)|k'> = \int d^3r\, e^{i(\vec{k'} - \vec{k})\cdot\vec{r}}\, u_k^*\, u_{k'}\, v(z) \tag{23}$$

If we make use of the fact that $A(k)$ is, by assumption, very strongly peaked at $k = 0$, we can approximate u_k and $u_{k'}$ appearing in Eq. (23) by u_o, their values at $k = 0$. Then $< k|v(z)|k' >$ is simply the Fourier transform of $|u_o(r)|^2\, v(z)$. Let's define $V(z) = |u_o(r)|^2 v(z)$ and call $V(k)$ its Fourier transform. Then Eq. (22) can be rewritten

$$[\varepsilon(k) - E]\; A(k) + \sum_{k'} V(k - k')\, A(k') = 0 \tag{24}$$

Now the introduce the envelope function $A(z)$ defined by

$$A(z) = \sum_k A(k)\, e^{ikz} \quad . \tag{25}$$

By taking the Fourier transform of Eq. (24) we find that the envelope function A(z) must satisfy the equation

$$\left[\varepsilon(-\, i\nabla) + V(z) - E\right] A(z) = 0 \tag{26}$$

This is just a one-dimensional Schrödinger equation for a particle of mass m_c in a potential V(z). The function $|u_o(z)|^2$ has the periodicity of the lattice and can therefore be expanded in the form

$$|u_o(z)|^2 = \sum_\kappa C_\kappa\, e^{i\kappa z} \quad , \tag{27}$$

where κ is a reciprocal latice vector. The only large term in the series will be the one with $\kappa = 0$ for the simple two band model we have employed, and we can approximate $|u_o(z)|^2$ by unity.

We can solve the Hartree problem analytically using a variational approach. Let's assume that the ground state eigenfunction $A_o(z)$ is of the form

$$A_o(z) \simeq \left(b^3/2\right)^{1/2} z\, e^{-bz/2} \tag{28}$$

This function vanishes at z = 0, the semiconductor-oxide interface, and falls exponentially to zero for large values of z. At low temperatures and moderate values of the gate voltage, only the lowest energy level of the surface potential well is occupied. Therefore the screening charge density of the inversion layer electrons is given by

$$\begin{aligned} N_s(z) &= N_{inv}\ |A_o(z)|^2 \quad , \\ &= \frac{1}{2}\, b^3\, N_{inv}\, z^2\, e^{-bz} \quad , \end{aligned} \tag{29}$$

where N_{inv} on the right hand side denotes the number of electrons per unit area in the inversion layer. By solving Poisson's equation and requiring the electric field to vanish at $z = \infty$ and the displacement

field to be continuous at $z = 0$, we obtain for $v(z)$

$$v(z) = \frac{4\pi e^2}{\varepsilon_s} \left\{ N_d z + N_{inv} b^{-1} \left[3 - e^{-bz}(3 + 2bz + \frac{1}{2} b^2 z^2) \right] + \frac{\varepsilon_s - \varepsilon_o}{16\pi(\varepsilon_s + \varepsilon_o)} z^{-1} \right\}. \tag{30}$$

In writing down Eq. (30) we have made the assumption that only the lowest eigenstate $\psi_o(z)$ is occupied. We now evaluate

$$< E > = < A_o(z) \left| \frac{p_z}{2m} + v(z) \right| A_o(z) > \quad , \tag{31}$$

and obtain

$$< E > = \frac{h^2 b^2}{8m} + \frac{12\pi e^2}{\varepsilon_s b} \left(N_d + \frac{11}{16} N_{inv} + \frac{\varepsilon_s - \varepsilon_o}{96\pi(\varepsilon_s + \varepsilon_o)} b^2 \right) \tag{32}$$

This is the energy of a single electron in the lowest subband. We want to minimize the total energy of the N_{inv} electrons per unit area with respect to the choice of the variational parameter b. Here we must be somewhat careful since the term involving N_{inv} in Eq. (32) is the interaction of the electrons with each other. If we simply add up Eq. (32) for each electron, we count the interaction term twice. Therefore, in minimizing the total energy of N_{inv} electrons per unit area, we replace the coefficient 11/16 appearing in front of N_{inv} in Eq. (32) by 11/32.

With this replacement minimization of the energy gives an equation for the variational parameter b

$$b^3 + \alpha b^2 = b_o^3 \quad , \tag{33}$$

where

$$b_o^3 = \frac{48\pi m e^2}{\hbar^2 \varepsilon_s} (N_d + \frac{11}{32} N_{inv}) \quad , \tag{34}$$

and

$$\alpha = \frac{1}{2} \frac{\varepsilon_s - \varepsilon_o}{\varepsilon_s + \varepsilon_o} \frac{me^2}{\hbar^2 \varepsilon_s} \tag{35}$$

For $b_o >> \alpha$ we can approximate the solution to lowest order in α and write

$$b \simeq b_o - \frac{1}{3}\alpha \quad . \tag{36}$$

Typical values of the parameters appropiate for a Si-100 surface inversion layer are: $\varepsilon_s = 11.7$, $\varepsilon_o = 3.9$, $m = 0.916\ m_o$, $N_d \simeq 10^{11}cm^{-2}$ and $N_{inv} \simeq 10^{12}cm^{-2}$. With these values we find $< E > \simeq 56.5meV$ above the bottom of the surface potential wells. This establishes the order of magnitude of the energies involved in the problem.

To obtain a more accurate estimate of the ground state and excited state energies as a function of N_{inv}, one must resort to numerical calculation. Stern[2] has carried out self-consistent Hartree calculations of the energy separations as a function of both N_{inv} and temperature. A fairly reasonable analytic approximation[14] can be made by introducing a sequence of variational functions $A_o(z)$, $A_1(z)$, ..,$A_n(z)$ where $A_n(z)$ has n-nodes at finite values of z and is orthogonal to all lower variational functions.

In figure 4 we present a schematic of the energy levels, wavefunctions and density of states of the first few bound states of the surface potential well. To the right we plot potential energy vs z, the coordinate normal to the surface. The semiconductor-oxide interface at $z = 0$ is taken to be an infinite barrier. The two lowest energy levels E_o and E_1 are indicated by horizontal lines and the envelope functions corresponding to them are indicated by the dashed lines. To the left we plot the density of states vs energy. At energies below E_o no states are available. Once E_o is reached, electrons begin to fill the two-dimensional $k_x - k_y$ space associated with free electron motion parallel to the surface. In two dimensions the free electron density of states is a constant, so D(E) jumps to that constant value at $E = E_o$; similar jumps appear every time a new level of the surface potential is reached.

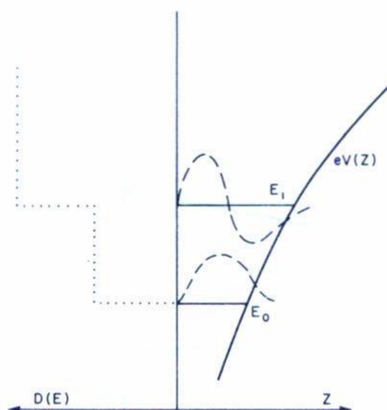

Fig. 4. Schematic of the energy levels and wavefunctions (dashed lines) of the first few bound states of the surface potential. To the left we plot the density of states as a function of energy. Each time a new quantum level occurs, the density of states experiences a jump to a new constant (two-dimensional density of states is independent of energy) value.

III. COMPARISON WITH EXPERIMENT

There have been a number of spectroscopic studies of the separation between the energy levels or subbands of the surface potential. In the first experiments[17] a change in the conductivity of the surface channel was observed when the frequency of the incident radiation was appropiate to cause transitions from the ground to the first excited subband. Later experiments[34] involved direct observation of the power absorbed by the quasi-two-dimensional electron gas of the surface inversion layer. Both of these experiments and later observations of intersubband luminescence gave information on energy separations of the subbands as a function of gate voltage or inversion layer concentrarion N_{inv}. A comparison[18] of the early experiments with the Hartree calculation is shown in Fig. 5. The solid curve is the Hartree energy separation, and the open circles are experimental results. Unfortunately, the agreement is not very good. The large discrepancy between the calculation and experiment is associated with the effects of exchange and correlation which are neglected in the Hartree approximation.

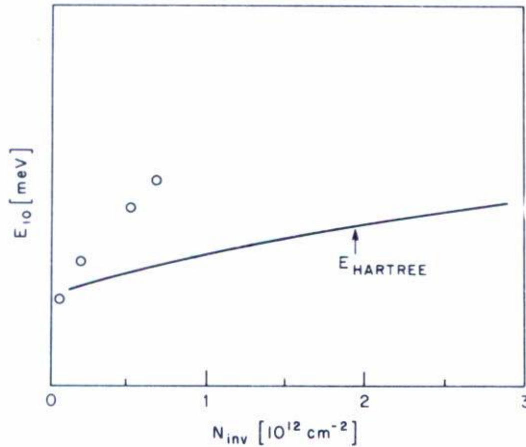

Fig. 5. A comparison of the calculated Hartree energy separation of the ground and first excited subbands vs N_{inv} with experimental results.

IV. ELECTRON-ELECTRON INTERACTIONS

Electrons in a semiconducting surface inversion layer have wavefunctions which extend of the order of 50Å from the semiconductor-oxide interface into the bulk of the semiconductor. The effective Coulomb interaction between the electrons (neglecting screening due to the other electrons in the inversion layer) is affected by the presence of the interface and the extent of the wavefunction normal to the surface. The effective unscreened interaction between a pair of electrons in the inversion layer is obtained by noting that a point charge located at the point (r', z') in the semiconductor sets up a potential $\phi(r - r'; z, z')$ at the point (r, z) in the semiconductor whose Fourier transform with respect to r - r' is given by[19]

$$\phi(q; z,z') = \frac{2\pi e}{\varepsilon_s q}\left\{ e^{-q|z - z'|} + \frac{\varepsilon_s - \varepsilon_o \coth q\delta}{\varepsilon_s + \varepsilon_o \coth q\delta}\, e^{-q(z + z')} \right\} \qquad (37)$$

This result is obtained from classical electrostatics by solving Poisson's equation in the semiconductor, the insulator, and the metal, and imposing the appropriate boundary conditions at the interfaces. If both z and z' are sufficiently small compared to q^{-1}, the potential is almost independent of z and z' and can be approximated by

$$\phi(q) \simeq \frac{2\pi e}{\varepsilon_s q} \frac{2\varepsilon_s}{\varepsilon_s + \varepsilon_o \coth q\delta} \tag{38}$$

This is the form of the interaction used by Chaplik[20] in studying the possibility of crystallization of the electrons into a two-dimensional Wigner lattice. For $\delta \gg q^{-1}$, $\phi(q)$ is approximately equal to $2\pi e/q\bar{\varepsilon}$, - where $\bar{\varepsilon} = \frac{1}{2}(\varepsilon_o + \varepsilon_s)$. This is the form of the interaction used in many microscopic calculations. The effective unscreened interaction between an electron in the nth level of the surface potential and one in the mth level is taken to be

$$V_{nm}(q) = -e \int dz\, dz' \, |\psi_n(z)|^2 |\psi_m(z')|^2 \, \phi(q; z, z'), \tag{39}$$

i.e., $\phi(q; z, z')$ is simply weighted by the probability of finding electrons at z and z'. If all the electrons are in the ground subband the unscreened interaction between them can be evaluated exactly

$$V_{oo}(q) = \frac{2\pi e^2}{\varepsilon_s q} I(q/b) \tag{40}$$

where the function I(x) is given by[19]

$$I(x) = (1 + x)^{-6} \left[\frac{1}{8}x\,(33 + 54x + 44x^2 + 18x^3 + 3x^4) + 2\varepsilon_s(\varepsilon_s + \varepsilon_o \coth q\delta)^{-1}\right] \tag{41}$$

and b is the variational parameter in the ground state wavefunction. V_{oo} differs from a two-dimensional Coulomb interaction by the factor I(q/b). For most purposes the oxide thickness δ is sufficiently large that $\coth q\delta$ can be replaced by unity for all significant values of q. In the limit that the inversion layer becomes very narrow ($b \to \infty$), I(q/b) reduces to $2\varepsilon_s(\varepsilon_s + \varepsilon_o)^{-1}$, giving for V_{oo} a two-dimensional Coulomb interaction with a dielectric constant $\bar{\varepsilon} = \frac{1}{2}(\varepsilon_s + \varepsilon_o)$.

In the most general case, the effective interaction between electrons in the inversion layer will depend on four subband indices. This dependence represents the fact that incident electrons in the i and ℓ subbands can scatter into the j and m subbands as depicted in Fig. (6a).

Electron Self-Energy

The many-body quasi-particle energy is the sum of the Hartree energy and the electron self-energy. Diagrammatic perturbation theory has been used by Vinter[6] to evaluate the electron self-energy at zero temperature, and more recently by Kalia *et al*[14] for finite temperatures. The diagrams depicting the self-energy calculation are shown in Fig. 6. The Green's function G_{ij} is represented by the double solid line shown in Fig. (6d), which is an integral equation for G_{ij}. The single solid line is the non-interaction Green's function G^o_{ij}, also shown in Fig. (6b). The non-interacting Green's function is actually diagonal in the subband indices, although the full Green's function G_{ij} isn't. The effective screened interaction (the double dashed line) between electrons is given by the equation depicted in Fig. (6c).

At finite temperature it is customary to define a self-energy function $M(z, z', \underline{k}, i\omega_n)$ over a discrete set of imaginary frequencies. The subband self-energies are defined by expanding M in the complete set of Hartree eigenfunctions $\psi_j(z)$. To lowest order in the effective interaction the i-j element of M is given by[14].

$$M_{ij}(\underline{k}, i\omega_n) = -\beta^{-1} \sum_{\ell} \sum_{\omega_m} e^{i\omega_m \eta} \int \frac{d^2p}{(2\pi)^2} U_{i\ell\ell j} (\underline{k} - \underline{p}, i\omega_n - i\omega_m) G^o_{\ell\ell}(\underline{p}, i\omega_m) \quad (42)$$

where the sum over ℓ runs over all subbands, and $\beta = (k_BT)^{-1}$. Here $G^o_{\ell\ell}$ is the non-interacting Green's function for the ℓth subband. Throughout this calculation we chose $\hbar = 1$.

From the Dyson equation for the effective interaction U we can obtain the relation

$$U_{ij\ell m} (\underline{k}, z) = V_{ij\ell m} (\underline{k}) + \int_{-\infty}^{\infty} \frac{d\omega'}{2\pi} \frac{f_{ij\ell m}(\underline{k};\omega')}{z - \omega'} \quad (43)$$

where z is a complex frequency, and $f_{ij\ell m}(k;\omega)$ is simply related to the imaginary part of $U_{ij\ell m}(k; z = \omega + i\eta)$. Here $V_{ij\ell m}(\underline{k})$ is the unscreened interaction between electrons in the inversion layer. Substituting Eq. (43) in Eq. (42) and performing the sum over ω_m, we find that M is a sum of exchange and correlation terms. The exchange part of self-energy, M^x_{ij},

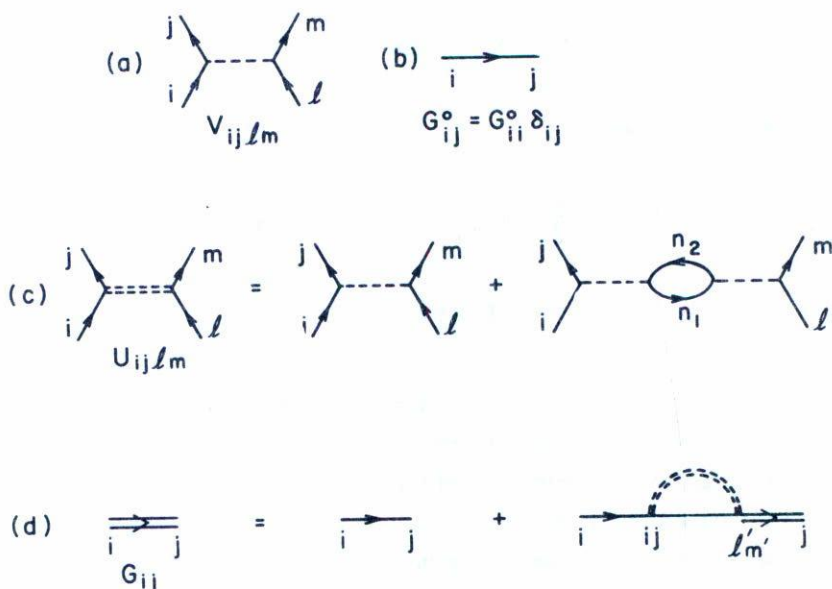

Fig. 6. (a) Schematic of the unscreened electron-electron interaction $V_{ijk\ell}$, represented by a dashed line.

(b) Noninteracting or bare Green's function $G^o_{ij} = \delta_{ij} G^o_{ii}$ represented by a solid line. This function is actually diagonal in the subband indices.

(c) Dynamically screened electron-electron interaction is represented by a double dashed line. It satisfies an integral equation depicted in the figure.

(d) The interacting or dressed Green's function G_{ij} is represented by a double solid line. It satisfies an integral equation depicted in the figure.

is given by

$$M^{x}_{ij}(\underline{k}) = -\sum_{\ell} \int \frac{d^2p}{(2\pi)^2} V_{i\ell\ell j}(\underline{p}) n_{\ell}(\underline{k} - \underline{p}) \quad , \qquad (44)$$

and the correlation part by

$$M^{c}_{ij}(\underline{k}, i\omega_n) = -\sum_{\ell} \int \frac{d^2p}{(2\pi)^2} \int_{-\infty}^{\infty} \frac{d\omega'}{2\pi} \left[i\omega_n - \omega' - E_{\ell} - \frac{1}{2} m_{\ell}^{-1} (\underline{k} - \underline{p})^2 + \mu \right]^{-1} \times$$

$$f_{i\ell\ell j}(\underline{p}, \omega') \left[n_{\ell}(\underline{k} - \underline{p}) + (e^{-\beta\omega'} - 1)^{-1} \right] . \qquad (45)$$

Here $n_{\ell}(\underline{k})$ is the Fermi function for an electron of energy $E_{\ell} + k^2/2m_{\ell}$, and μ is the chemical potential of the system.

Explicit calculations for the bare interaction reveal that $V_{ij\ell m}$ has a significant contribution only if $i = j$ and $\ell = m$. Under these conditions, the self-energy M becomes diagonal. For convenience, we denote M_{ii} by M_i, V_{iijj} by V_{ij}, and f_{iijj} by f_{ij}.

The calculation of exchange energy is straightforward. For the evaluation of $M^{c}_{i}(\underline{k}; i\omega_n)$ we need the imaginary part of the retarded effective interaction, f_{ii}. The latter is calculated in the plasmon pole (pp) approximation[21,22]. We make the ansatz that for $\omega > 0$

$$\mathrm{Im}\, \varepsilon^{-1}_{ij}(\underline{k}, \omega) = C_{ij}(\underline{k})\, \delta(\omega - \omega_k) \quad , \qquad (46)$$

where ε_{ij} is an element of the dielectric matrix, ε, defined by $\varepsilon \cdot U = V$. Substituting $U = \varepsilon^{-1} \cdot V$ in Eq. (43) and letting $z = \omega + i\eta$ we obtain the Kramers-Kronig relations between the real and imaginary parts of ε^{-1}. Taking the RPA expression for the real part of ε^{-1}, we determine $C_{ij}(\underline{k})$ and ω_k from the static limit of the Kramers-Kronig relations and the f-sum rule. From the knowledge of C_{ij} and ω_k we obtain $\mathrm{Im}\varepsilon^{-1}_{ij}$ and subsequently f_{ii}.

The quasi-particle energies are the solutions of Dyson's equation. Rice[23] has pointed out that if the self-energy is evaluated only to lowest order in effective interaction, it is inappropriate to solve the exact Dyson equation since it generates not only the lowest order terms in effective interaction, but also selected higher order terms which should

not be included in the calculation. Instead, the self-energy should be evaluated at a frequency corresponding to the noninteracting quasi-particle energy, that is

$$\omega_i(\underline{k}) \simeq E_i + \frac{1}{2} m_i^{-1} k^2 - \mu + \text{Re}\, M_i(\underline{k}; E_i + \frac{1}{2} m_i^{-1} k^2 - \mu) \qquad (47)$$

The quasi-particle energies $E_i^*(\underline{k})$ are then given by $\omega_i(\underline{k}) + \mu$.

We have evaluated the exchange and correlation parts of the self-energy as a function of temperature at several values of the inversion layer concentration for the three subband model. A comparison of the quasi-particle separation $E_1 - E_0$ including exchange-correlation effects with the Hartree energies and with experiment is given in Fig. 7 for the case of zero temperature. Clearly the effects of exchange and correlation are very important, and they bring the theoretical calculations much closer to the observed energy separations.

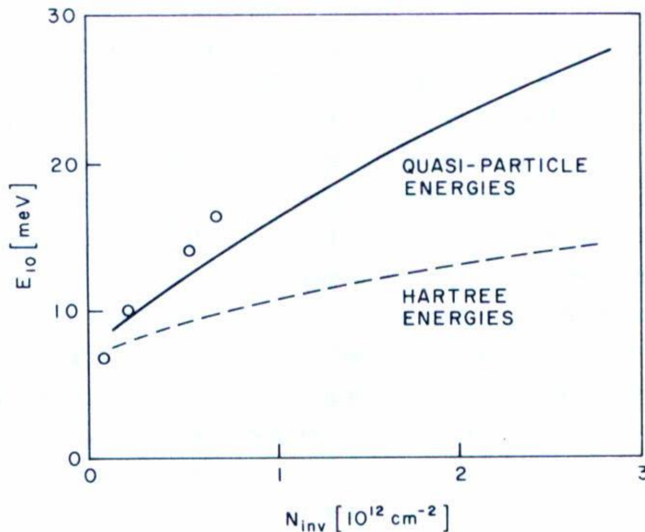

Fig. 7. A comparison of Hartree energy separations and many-body quasi-particle energy separations vs N_{inv} with experiment for the case of zero temperature. These results are taken from the work of Vinter[18].

The material most commonly studied has been silicon. The conduction band of silicon has six minima located along the 100 directions approximately 85% of the wave vector from the zone center to the face of the Brillouin zone. The constant energy surfaces are ellipsoids of revolution about the 100 axis on which the minimum is located. The effective mass along the direction of the axis of revolution is large ($m_z \simeq 0.96\ m_0$) while the mass in the direction normal to the axis is small ($m_\perp \simeq 0.19\ m_0$). For a silicon 100 surface inversion layer the two ellipsoids whose heavy-mass axis is normal to the surface form the lowest energy level of the surface potential. The lowest energy level of the four ellipsoids whose light-mass axis is normal to the surface is higher in energy. Because of this structure of the conduction band of silicon, the surface electric subbands fall into two groups. The labels 0, 1, 2,... on the subbands denote the ground, first excited, second excited,... subbands of the two heavy-mass ellipsoids. The labels 0', 1',... denote the subbands of the four light-mass ellipsoids.

According to the self-consistent Hartree calculation most of the electrons reside in 0, 1, and 0' subbands, therefore in the temperature range of interest, the 3-subband model is expected to be a reasonable approximation. Figure 8 illustrates the variation of self-energies of 0, 1, and 0', subbands with temperature. At low and intermediate temperatures the main contribution to the self-energy of the 0th subband comes from exchange. The small size of M_0^c results from the large cancellation between the first and second terms in the parenthesis of Eq. (45). As the temperature increases, the population in the 0th subband decreases; this results in a decrease in the exchange energy and an increase in the correlation contribution to the self-energy. At extremely high temperature, the self-energy becomes very small indicating that the system approaches the classical limit. The exchange energy for the excited subbands is very small at low and intermediate temperatures; the main contribution comes from the correlation part. For these subbands almost no cancellation occurs between the two terms in the parenthesis of Eq. (45), because the first term has a negligible value at low and intermediate temperatures. With increase in temperature, the exchange contribution grows and the correlation part diminishes. Finally, at very high temperatures,

the total self-energies for the 0' and 1 subbands become very small. It should be observed that the self-energies for the 0' and 1 subbands show a remarkably similar dependence on temperature.

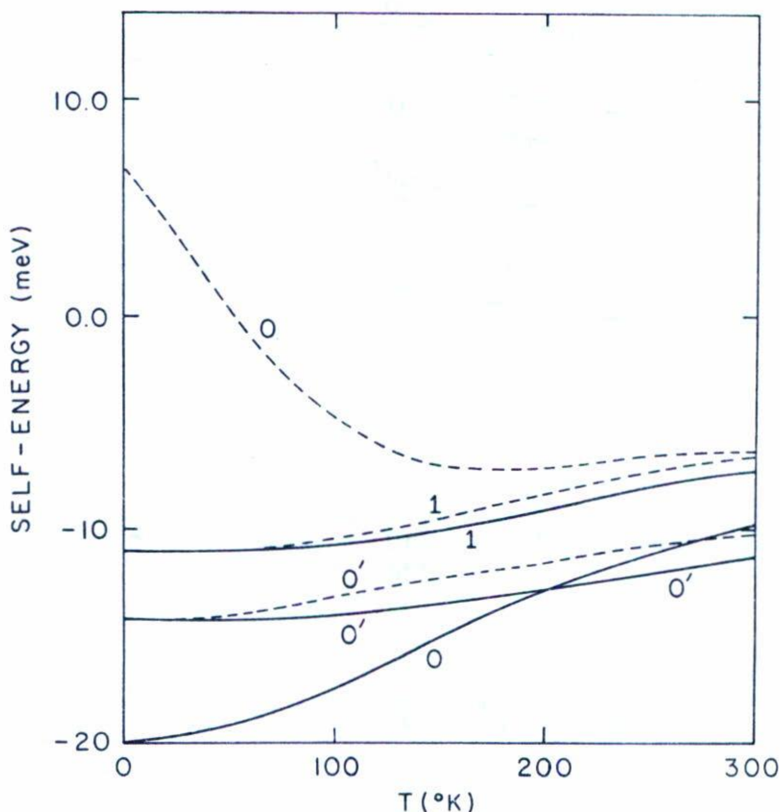

Fig. 8. Temperature dependence of the self-energies (solid lines) and exchange energies (dashed lines) of the 0, 1 and 0' subbands of a Si-100 surface inversion layer.

In Fig. 9 we display the quasi-particle energies at the subband minima as a function of temperature for $N_{inv} = 10^{12}/cm^2$. For very low concentrations ($N_{inv} \simeq 10^{11}/cm^2$) the subband separations turn out to be almost independent of temperature. At higher concentrations they increase slightly with increasing temperature. The exchange-correlation energies are quite insensitive to the value of the wave vector $\underline{k}$ parallel to the surface, so that the self-energy effects produce only a rigid shift in the subbands.

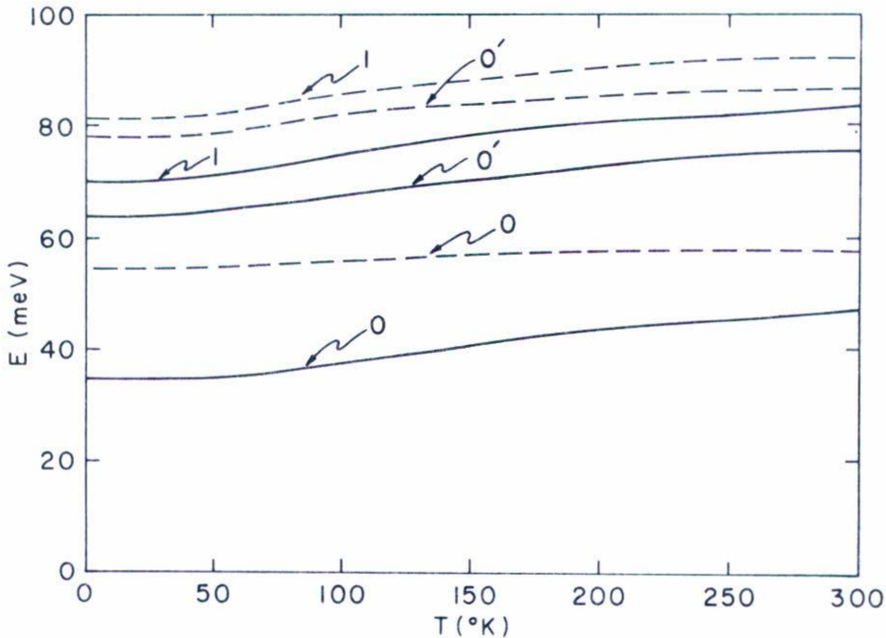

Fig. 9. Temperature dependence of the quasi-particle energies at $k = 0$ for the 1, 0 and 0' subbands. These energies are calculated for $N_{inv} = 10^{12} cm^{-2}$ and $N_d = 3.2 \times 10^{11} cm^{-2}$.

V. DEPOLARIZATION EFFECT AND VERTEX CORRECTION

In comparing the calculated subband separations with experiments on optical absorptions or luminescence, two important effects have been neglected. These effects are the resonance screening[24,25,26] (or depolarization shift) and the final state interaction[15] (or vertex correction or exciton effects). The physical processes associated with these two effects are shown in Fig. 10. Fig. 10a shows the process associated with intersubband absorption in the Hartree approximation. An electron is excited to the nth subband leaving a hole behind in the ground subband. The inclusion of exchange-correlation effects in the quasi-particle energies simply replaces the bare Green's functions of the Hartree approximation by the dressed Green's functions represented by the double solid

line of Fig. 10b. The depolarization shift or resonant screening effect results from the processes shown in Fig. 10c. The dynamic polarizability of a noninteracting two level system (0 and 1 subbands) is given by

$$\chi_{10}^{(o)}(q = 0, \omega) = \frac{2N_{inv}E_{10}}{\omega^2 - E_{10}^2} \tag{48}$$

where E_{10} is the energy separation between the 0 and 1 levels and N_{inv} is the number of electrons in the inversion layer. The diagram corres-

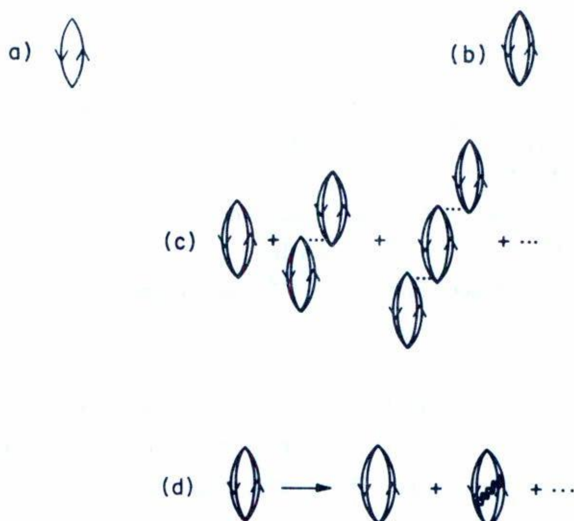

Fig. 10. (a) Intersubband absorption in the Hartree approximation. An electron in an excited subband is created and a hole left behind in the ground subband due to absorption of an incident photon.

(b) Same process as in (a) except that dressed Green's functions are used in place of the bare Green's functions of the Hartree approximation.

(c) In the absorption process not just single electron-hole pair creation must be considered, but the infinite chain of processes depicted in the figure must be included.

(d) The first order correction to the polarizability associated with final state interaction or vertex correction.

ponding to this polarizability is Fig. 10a in the Hartree approximation or 10b when the electron self-energies are included. However, the resonances in the infrared absorption do not occur at the poles of $\chi_{10}^{(o)}$, because the incident radiation polarizes the electron gas. This means that the entire infinite chain of polarization bubbles must be included in the response function. The full response function χ_{10} can be calculated by summing this series; we obtain

$$\chi_{10}(q = 0,\omega) = \frac{\chi_{10}^{(o)}(q = 0,\omega)}{1 - V_{1010}(q=0)\, \chi_{10}^{(o)}(q = 0,\omega)} \qquad (49)$$

where V_{1010} represent the scattering of an electron from 0 to 1 due to the Coulomb interaction. It is easy to see that the poles of χ_{10} occur at $\omega = \sqrt{E_{10}^2 + 2N_{inv} E_{10} V_{1010}}$ instead of at $\omega = E_{10}$. This is referred to as the depolarization shift.

The effect of final state interaction or exciton shift arises from the interaction between the excited electron and the hole which it leaves behind in the ground subband. Ando[15] has investigated this effect using a density functional approach. He neglects the wavevector and frequency dependence of the vertex correction, and finds qualitatively that the exciton-like shift tends to cancel the depolarization shift. Kalia *et al*[27] have studied the vertex correction by evaluating the first order correction $\chi_{10}^{(1)}(q = 0,\omega)$. This orrection is shown in Fig. 10d as the replacement of $\chi^{(o)}$ by $\chi^{(o)} + \chi^{(1)}$. These authors find that in the plasmon pole approximation there is a very large cancellation between the depolarization shift and the vertex correction. Their results for the -- $0 \rightarrow 1$ and $0 \rightarrow 2$ transitions as a function of N_{inv} are shown in Fig. 11. The dashed curves are the quasi-particle energy differences. For all values of N_{inv}, the value of $\pi_{10}^{(1)}$ is very small compared to $\pi_{10}^{(o)}$ at the resonance energy, so that stopping at the first order correction is reasonable. Because the resonance energies and quasi-particle separations are so close together, it appears to be adequate to use the calculated values of the quasi-particle energies in a comparison of theory and optical experiments. The large degree of cancellation between the depolarization shift and vertex correction has been demonstrated only for the case of zero temperature. However, if we go ahead and compare the quasiparticle separations at finite temperature with the result of Koch and Kneschaurek[11] we obtain reasonable qualitative agreement.

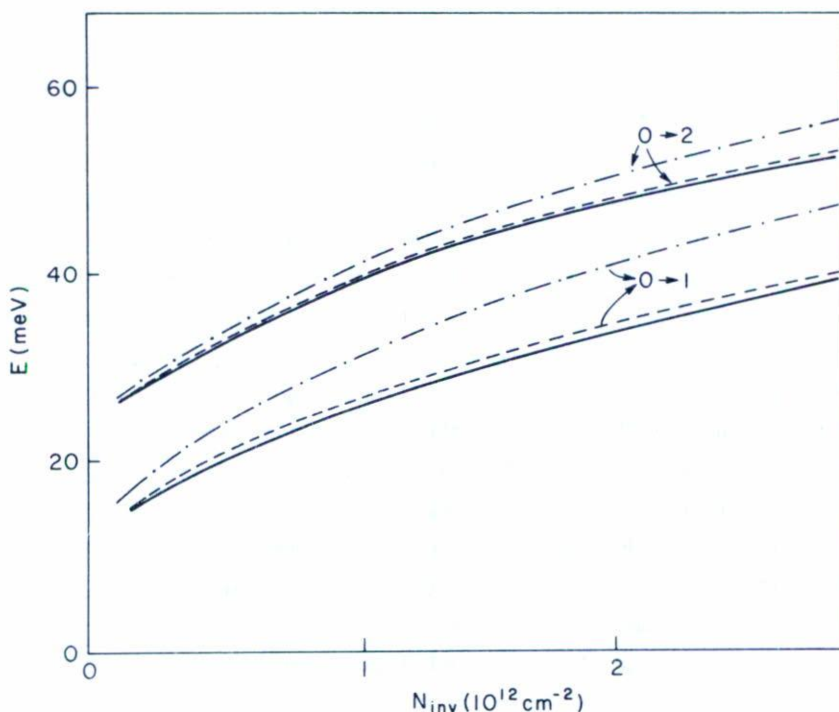

Fig. 11. The quasi-particle energy difference E_{10} and E_{20} as a function of N_{inv} are shown as dashed curves. These are compared with the positions of the resonance absorption peaks if only the depolarization effect is included (dot dashed curve) and when both depolarization and final state interactions are included (solid curves). The solid curves are always very close to the quasi-particle separations, showing that the depolarization shift and vertex correction tend to cancel. These calculations are performed with $N_d = 3.2 \times 10^{11} cm^{-2}$.

The evaluation of the vertex correction at finite temperature is a difficult numerical problem, and we have no justification for assuming the depolarization shift-vertex correction cancellation will continue to hold at finite temperatures. It would be very useful to have an independent measurement of the quasi-particle separations in which no depolarization or vertex correction effects occurred. The next section discusses one possible experiment of this type.

VI. SURFACE CHANNEL TUNNELING

We propose a potentially very useful new method of subband spectroscopy which involves tunneling into the surface channel[16].

The basic idea of a surface channel tunnel junction (SCTJ) is presented in the following three figures. In Fig. 12 the normal MOSFET structure is shown. In Fig. 12a degenerate n-type source and drain contacts at the surface of a weakly p-type semiconducting substrate are shown. This structure is separated from a conducting gate electrode by an insulating (here shown as oxide) layer. The band structure just inside the semiconductor as a function of position along a line parallel to the interface is shown in Fig. 12b for the case when no gate voltage is applied across the insulating layer. The Fermi level is shown as a dashed horizontal line. In the degenerate n-type regions the Fermi level is above the conduction band edge, while in the p-type substrate it is just slightly above the valence band edge. At very low temperatures no carriers are present in the substrate, and it behaves like an insulator. The -- highest energy occupied states in each region are indicated by the cross hatching. Figure 12c shows the band structure along the same line just inside the semiconductor when a gate voltage large enough to produce a surface inversion layer is applied. Now the two degenerate n-type contacts are connected by a conducting surface channel. In Fig. 13 the energy bands along a line perpendicular to the interface are shown for the surface channel depicted in Fig. 12c. Near the semiconductor-oxide interface, the conduction band edge is below the Fermi level as was shown in Fig. 12c. The energy bands are bent in the vicinity of the surface by the self-consistent field of the depletion charge and the inversion layer electrons. The motion of the electrons in the surface channel in the direction normal to the surface is quantized, and a sequence of electric subbands is formed. Within a given subband each electron is in the same quantum mechanical state of motion perpendicular to the surface, but acts as a free electron with respect to the degrees of freedom parallel to the surface. Thus, each subband acts like a quasi-two-dimensional electron gas.

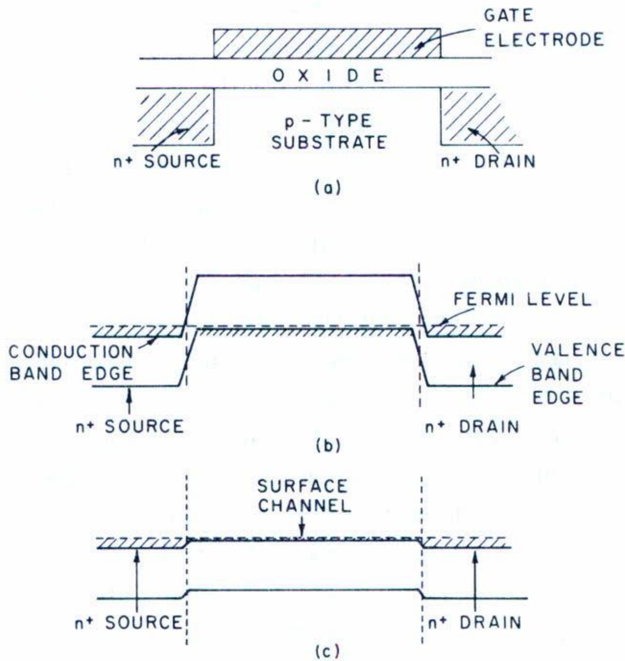

Fig. 12. Normal MOSFET configuration. Degenerate n-type source and drain contact are diffused into a weakly p-type substrate. The conducting gate electrode is separated from the semiconductor by an insulating layer as shown in (a). (b) and (c) show the band structure as a function of position along a line parallel to the interface but just inside the semiconductor for the case of zero gate voltage and a large gate voltage respectively. In (c) a conducting surface -- channel (the surface inversion layer) connects the source and drain contacts.

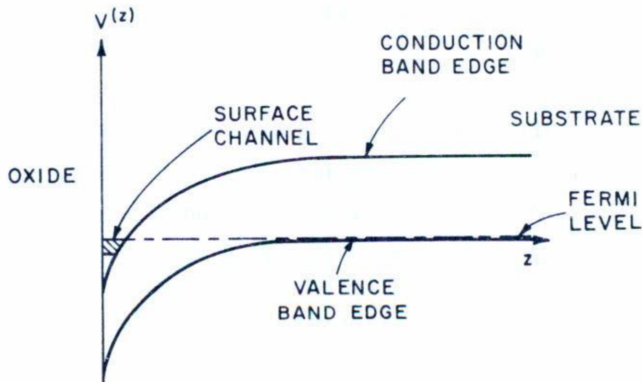

Fig. 13. The band structure along a line normal to the interface for the case of a surface channel as shown in figure 12c.

One type of SCTJ structure[28] is shown in Fig. 14. In Fig. 14a we have simply replaced the degenerate n-type source contact by a metallic contact which forms a Schottky barrier with the semiconductor. In practice the metallic contact is chromium silicide or platinum silicide which is formed by evaporating the transition metal onto the silicon wafer and heating at a prescribed temperature for an appropriate length of time. The band structure along a line just inside the semiconductor is shown in Fig. 14b for the case of zero gate voltage. Both the source and drain contacts are highly conducting, but the substrate is insulating at low temperature. In Fig. 14c, we show the same band structure for the situation in which the applied gate voltage is large enough to create a surface inversion layer. Now the conducting surface channel is separated from the metallic source electrode by a Schottky barrier tunnel junction.

The tunnel junction connects what is essentially a three-dimensional metallic source with a quasi-two-dimensional n-type surface channel. When a source-drain voltage is applied across the device, almost the entire voltage drop will appear across the tunnel junction. Fig. 15 shows a situation in which only the lowest subband of the surface channel is occupied. As soon as a voltage is applied such that the Fermi level in the source region is higher than in the surface channel, electrons can begin to tunnel from the source into unoccupied states of the ground subband. In direct specular tunneling both energy and the component of wavevector parallel to both the surface and to the juction will be conserved. The tunneling probability will depend upon the overlap in the direction normal to the surface of the wave function for the subband with the wave functions of the electrons in the source region. The tunnel current from the source into the ground subband should be a continuous function of the applied source-drain voltage. At the voltage V_1 however, a new process, tunneling into the first excited subband, becomes possible. The occurrence of this new tunneling proces should lead to breaks in the conductance dI/dV_{SD} as a function of the source-drain voltage V_{SD}. The applied source-drain voltage at which the nth discontinuity in the slope of conductance occurs should be equal to the energy separation of the nth subband and the ground subband less the Fermi energy of the surface channel (measured from the minimum of the ground subband). Thus by studying the I-V characteristics as a function

of both V_{SD} and V_{gate}, the dependence of the subband separation on electron concentration can be determined experimentally. If readily tunnelable SCTJ's can be prepared, this technique offers a very powerful means of studying many-body effects in quasi-two-dimensional systems.

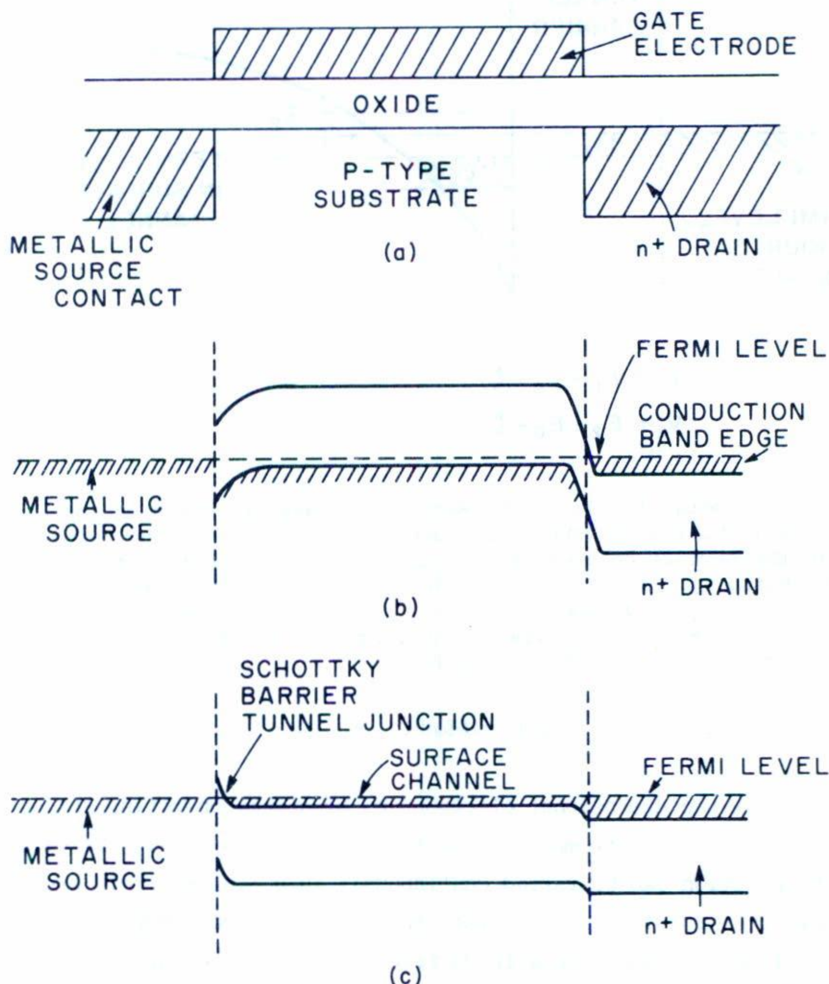

Fig. 14. One possible SCTJ configuration. A metallic source electrode replaces the degenerate n-type source contact of figure 12. A Schottky barrier is formed between the metallic source contact and the bulk p-type silicon as shown in (b). When a large gate voltage is applied, the Schottky barrier between the gate electrode and the surface channel forms the tunnel barrier as shown in (c).

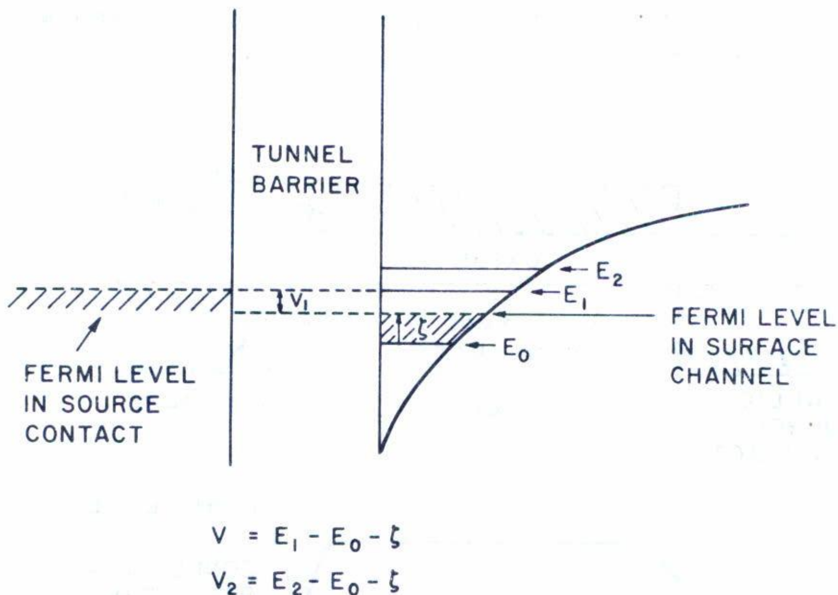

Fig. 15. The energy levels of the surface channel are shown on the right. Only the lowest subband is taken to be occupied. The Fermi level in the surface channel is a distance above the bottom of the ground subband E_0. The Fermi level in the source is indicated to lie a distance V_1 above the Fermi level in the surface channel. At this applied source-drain voltage tunneling into the first excited subband becomes energetically possible.

VII. SUMMARY

The quasi-two-dimensional electron gas of a semiconducting surface inversion layer is an extremely interesting many-body system. The electron concentration can be varied continuously in a single sample over a wide range of values; because of this the relative importance of exchange-correlation in comparison with Hartree effects can be varied. In the present paper we have investigated the simplest many-body theory. The electron self-energy has been calculated only to the lowest order in the dynamically screened interaction. Comparison of Hartree energy separations with many-body quasi-particle energy differences demonstrates how large the exchange-correlation effects are.

The problems involved in comparing the calculated quasi-particle separations with experimental data on optical absorption has been dis-

cussed. The depolarization shift tends to increase the resonance energy above the quasi-particle separation by an amount proportional to the electron concentration. The vertex correction or final state interaction has been studied in the plasmon-pole approximation, but only the lowest order correction term has been evaluated, and only for the case of zero temperature. We obtain a very large cancellation between these two -- effects, so that the quasi-particle separations are quite close to the resonance energies observed experimentally. This is in qualitative agreement with results obtained by Ando, although the methods of calculation and approximations used are very different. We have not carried out a calculation of the vertex correction at finite temperatures.

The possibility of directly observing the quasi-particle separations by the technique of surface channel tunneling has been described. This technique may prove to be a very useful method of probing the electronic structure of semiconducting surface inversion layers.

ACKNOWLEDGEMENT

The author would like to acknowledge the assistance of Drs. Rajiv Kalia and Sankar Das Sarma. A number of results quoted in this paper have been taken from their work, and the author has benefitted from numerous discussions with them.

REFERENCES

1. F. Stern and W.E. Howard, Phys. Rev. 163 (1967) 816.
2. F. Stern, Phys. Rev. Lett. 21 (1968) 1687; Phys. Rev. B5 (1972) 4891.
3. A. Kamgar, P. Kneschaurek, G. Dorda and J.F. Koch, Phys. Rev. Lett. 32 (1974), 1251.
4. A. Kamgar, P. Kneschaurek, W. Beinvogl and J.F.Koch, Proc. of the 12th Int. Conf. on the Physics of Semicondcutors, Stuttgart, West Germany 1974. B.G. Teubner, Stuttgart(1974) p. 709.
5. F. Stern, Phys. Rev. Lett. 30 (1973) 278.
6. B. Vinter, Phys. Rev. Lett. 35 (1975) 598.
7. T. Ando, Phys. Rev. B13 (1976) 3468.
8. P. Hohenberg and W. Kohn, Phys. Rev. 136 (1964) B864.
9. W. Kohn and L.J. Sham, Phys. Rev. 140 (1965) A1133; Phys. Rev. 145 (1966) 561.
10. R. Kalia, S. Das Sarma, M. Nakayama and J.J. Quinn, Phys. Rev. B18 (1978) 5564.
11. P. Kneschaurek and J.F. Koch, Phys. Rev. B16 (1977) 1590
12. See, for example, F.J. DiSalvo, Surface Science 58 (1976) 297.

13. M.J. Kelly and L. Falicov, Phys. Rev. Lett. 37 (1976) 1021, and Phys. Rev. B15 (1977) 1974 and 1983.
14. R. Kalia, S. Das Sarma, M. Nakayama and J.J. Quinn, to be published.
15. T. Ando, Z. Physik B26 (1977) 263.
16. J.J. Quinn, G. Kawamoto and R.B. McCombe, Surf. Science, 73 (1978) 190.
17. R.G. Wheeler and H.S. Goldberg, IEEE Trans. Electron Devices ED-22, (1975) 1001.
18. B. Vinter and F. Stern, Surface Science 58 (1976) 141.
19. T.K. Lee, C.S. Ting and J.J. Quinn, Solid State Comm. 16 (1975) 1309.
20. A.V. Chaplik, Soviet Physics - JETP 33 (1971) 997.
21. B.I. Lundquist, Phys. Kondens.Mater. 6 (1967) 193 and 206.
22. A.W. Overhauser, Phys. Rev. B3 (1970) 1888.
23. T.M. Rice, Ann. Phys. 31 (1965) 100.
24. W.P. Chen, Y.J. Chen and E. Burstein, Surf. Sci. 58 (1976) 263.
25. S.J. Allen, C.D. Tsui and B. Vinter, Solid State Commun. 20 (1976) 425.
26. M. Nakayama, Solid State Commun. 21 (1977) 587.
27. R. Kalia, S. Das Sarma, M. Nakayama and J.J. Quinn, to be published.
28. R. Kaplan, B.D. McCombe and J.J. Quinn, to be published.